THE ASTRONOMICAL JOURNAL VOLUME 104, NUMBER 4 OCTOBER 1992

[O II] AND CONTINUUM STRUCTURE IN RADIO-LOUD QSOs TO z=0.9

J. B. HUTCHINGS[1]

Dominion Astrophysical Observatory, NRC of Canada, 5071 W. Saanich Rd, Victoria, B.C. V8X 4M6, Canada

Received 12 March 1992; revised 21 May 1992

ABSTRACT

Images have been obtained in R band and redshifted 100A band [O II] with the High Resolution Camera of the Canada–France–Hawaii Telescope. Ten quasi-stellar objects were observed, with redshifts from 0.36 to 0.91, with radio structures ranging from unresolved to large double-lobed. The images have a mean full width at half maximum 0.64 arcsec, and a spread from 0.45 to 0.80. Extended emission line structure is seen in all cases, with a variety of properties. In particular, in four of the six large radio sources, the emission line gas appears to be associated with the radio structure. However, the connection between radio and emission line structure is not as marked as in radio galaxies, and no large emission line regions are seen. The continuum images are resolved in six of the nine cases, four of which are at redshifts larger than 0.8. The evolution of the sources is discussed.

1. INTRODUCTION AND OBSERVATIONS

Stockton & MacKenty (1987) investigated a sample of low redshift quasi-stellar objects (QSOs) by obtaining images in appropriately redshifted [O III]. They found that 15 of 47 of their sample have extended line emission, which generally have irregular morphologies which bear little resemblance to the host galaxy structure. The sample contained 26 radio-loud and 21 radio-quiet QSOs. Of the 15 with extended line emission, 11 are radio-loud, and the emission is stronger in the steep-spectrum sources. In the few cases with detailed radio maps, there is a weak correspondence between the radio and emission-line structure. These clouds of gas are probably the result of the tidal effects that have led to the nuclear activation, but it is not clear whether the line radiation traces all the gas, or only that which is illuminated by beamed or shielded nuclear radiation.

In more recent work at higher redshifts, it has been found that there is a remarkable correspondence between the radio and optical line emission structure in the strong 3C radio sources, particularly at $z>0.8$ (McCarthy *et al.* 1991; McCarthy 1991). The correspondence is seen in both radio galaxies and radio QSOs, although the galaxies have been more extensively investigated, and the result is weaker for the QSOs. The correspondence between the radio and optical line gas is (a) alignment with the radio source structure; (b) stronger line emission on the side of the shorter radio lobe; and (c) correlation of the radio and emission line fluxes. These results very strongly indicate that there is a connection between the gas and the radio plasma, and suggest that the radio activity is one-sided. This has lead to more than one scenario for the connection: for example that the radio jet excites star formation in pre-existing gas clouds, or alternatively that the jet entrains material and carries it to remote sites. The gas may be excited by beamed radiation along the radio axis or it may be powered by local star formation. The existence of the effect increasingly at higher redshifts indicates a cosmic evolution, perhaps in the amount of gas in the young galaxy or in the IGM in which it lives. The connection between radio and optical morphology raises many interesting questions and offers the opportunity of understanding structures at early cosmic epochs.

At high redshifts (2 and higher), Heckman *et al.* (1991) have resolved Lyα and continuum (UV rest frame) images of QSOs. In many cases they find that the line emission is large and luminous and aligned with the radio structure. The continuum (stellar?) flux is not so aligned. These results are less detailed but similar to the radio galaxy and lower redshift results.

In other recent work, Neff & Hutchings (1990, and references therein) have investigated the radio structure of QSOs at redshifts from 0.4 to 3.7. These studies have suggested that radio structure grows on one side at a time, and have shown that at early epochs the sources spent less of their lifetime as large double-lobed structures than at low redshifts. The observed range of structures result from the combination of individual source evolution and the cosmic evolution of structure types. Thus, the youngest sources are unresolved, structure grows first on one side, and the activity then switches direction to grow on the other side. This alternating ejection may continue, or have only one reversal. The association of optical line emission with the shorter radio lobe is consistent with this scenario, and may offer significant insight into the growth of radio structure.

Since the observations to date have concentrated on the steep spectrum (lobe dominated) sources of high luminosity, they have not investigated this source growth scenario. The present observations were made to extend the data on line emission to radio sources of *lower power and particularly to sources with smaller, one-sided, and unresolved structure.* A full investigation calls for a good sampling of redshift, radio power, and radio structure parameters, and will need a large amount of observing time. Thus, the

[1]Guest Observer, Canada–France–Hawaii telescope, which is operated by NRC of Canada, CNRS of France, and the University of Hawaii.

TABLE 1. Data.

Name	z	m	Size (Kpc)	20cm(logW/Hz) core	lobe	λ_z (A)	λ_{obs}/trans[a] (A)/%	Exp R/NB (secs)	FWHM (")
0738+313	0.63	16.1	U	27.2	-	6078	6104/54	600/1800	0.57
0903+169	0.41	18.3	160	24.4	26.4	7065[b]	7090/55	600/2400	0.60
0957+003	0.91	17.6	170	26.1	27.2	7107	7090/56	600/2400	0.56
1022+194	0.83	17.5	60	26.9	26.6	6813	6809/61	600/1950	0.66
1104+167	0.63	15.7	190	26.3	26.7	6090	6104/50	600/2400	0.70
1151+102	0.90	18.4	U	26.5	-	7063	7090/54	600/2700	0.45
1253+104	0.83	18.2	130	25.7	26.7	6798	6809/59	600/2700	0.59
1340+289	0.91	17.1	11[c]	26.4	26.5	7100	7090/57	600/1800	0.80
1423+242	0.65	17.2	100	25.8	27.1	6146	6104/42	600/1800	0.72
1510−089	0.36	16.5	29[c]	26.6	25.5	6815[b]	6809/62	300/2400	0.78

[a] Filter transmission at emission line wavelength

[b] 5007A line imaged

[c] one-sided radio structure

Size assumes $H_0=100$ $q_0=0.5$

U=unresolved (<0.4" at 6cm)

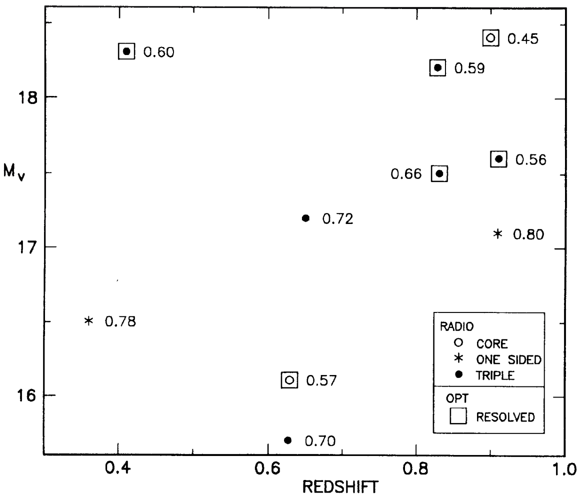

FIG. 1. Redshift and magnitude of sample QSOs, showing radio morphology types. The numbers are the image FWHM in arcsec. Squares indicate objects resolved in the continuum image. All objects are resolved with FWHM better than 0.7 arcsec, and fainter objects are more easily resolved.

present results represent an initial exploration, and it is difficult to draw statistical conclusions from the results.

The sample observed was drawn from the list of radio QSOs mapped in detail by Hutchings *et al.* (1988, hereafter referred to as HPG), attempting to cover the range of source sizes, with some range in redshift and source power. The objects observed were also strongly constrained by the observing season and the weather. Table 1 shows the objects observed. It was intended to include at least one object also observed by McCarthy and van Breugel, but this was not done because weather restricted the observing time.

The observations were obtained in Feb 1991 using the HR Camera (McClure *et al.* 1989) at the Canada–France–Hawaii telescope (CFHT). HR Cam was chosen as the sources are at high redshift compared with previous imaging programs, the radio source sizes did not require a large field, and considering the possibility that the [O II] gas may have very sharp structure. In order to have a reasonable sized shopping list of targets, the narrow-band filters used were 100A bandpass, which is significantly wider than the line emission expected. The observed wavelengths were near to 7000A, the redshifted wavelength for [O II] 3727A for most sources. For the two lower redshift objects, the observed wavelength corresponded to redshifted [O III] 5007A.

The detector used was the SAIC 1024^2 pixel charge-coupled device (CCD), which samples the sky at intervals of 0.13 arcsec with the HR Camera. The read noise is about 6e, and there is a faint 2e pattern in the images (from AC mains interference) which could not be fully removed and is visible in the images with weak signal. The continuum observations were made with the *R* band filter for all the objects. Exposures were generally 10 min for the *R* band and 30–45 for the narrow band. This did not allow very deep detections, but was adopted as the best compromise to observe several objects of different types in the time available. All observations used the nearest good guide star, which ranged from 20 to 90 arcsec away. Table 1 lists the observational details, and the measured image full width at half maximum (FWHM) from stars in the field. The weather during the run was variable, and the image quality has a wide range. While all data have subarcsecond resolution, only one object was seen with images close to the best (0.4 arcsec) obtainable with the camera. In terms of the detection of line emission this is not critical, but for continuum band resolution of the host, it is.

Continuum band flux calibrations were obtained from observations of a standard star field. The same fields were observed with the NB filters, to yield a continuum magnitude calibration for them. The filter transmission curves were used as a check on these data, and found to be consistent. No emission-line flux standards were observed, so that the transformations to emission-line flux which are quoted later, are derived from these continuum source observations. In Table 1 we show the transmission of the NB filters at the wavelengths of the lines (redshifted by the same as the QSO itself). In all cases this value is within 10% of the filter peak: the lines were not situated in the steep wings of the filter transmission curves.

The data were processed using standard IRAF software. The continuum images were scaled to remove the stars in the field in subtracting them from the narrow-band data. A "continuum equivalent" calibration for the narrow-band filters was derived from the standard star field data, and the scale factors were found to be close to the numbers expected from the filter transmission data. This is discussed in more detail below.

2. CONTINUUM IMAGES

While they are not very deep, the broad-band continuum images generally have good spatial resolution, and they were investigated for extended structure and companion objects to the QSOs. Figure 1 shows the objects observed on the redshift/magnitude plane, and also shows which are optically resolved. To do this, the QSO luminosity profiles were compared with star profiles from the same frame, and the images carefully inspected and contoured

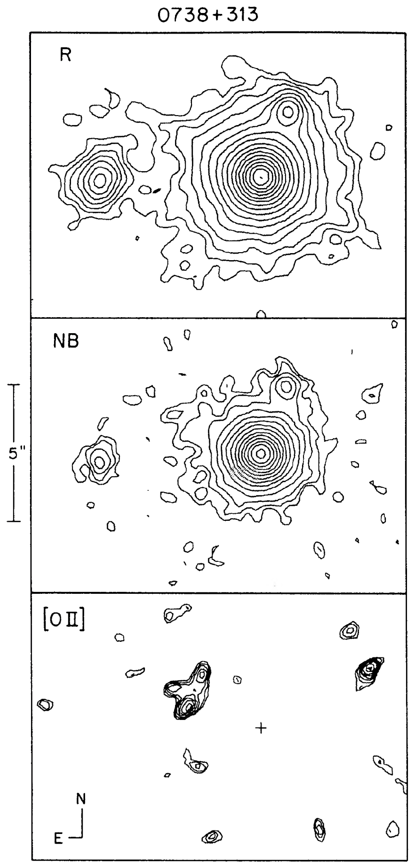

FIG. 2. Images of 0738+313. The [O II] image is continuum-subtracted. The diagonal structure in the *R* image is the telescope diffraction spike. Contour levels in *R* and NB are equal factors apart; in the [O II] image they are equal linear intervals. The radio source is unresolved at 0.4 arcsec.

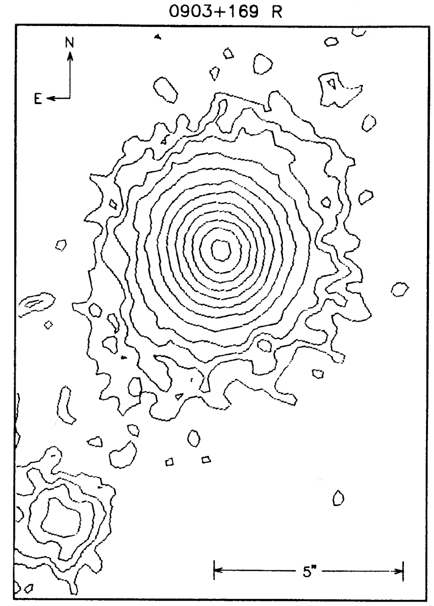

FIG. 3. *R* band image of 0903+169. Contours are equal factors apart.

for low light level features. We describe below the details for the individual objects. In this section we also discuss the structure of the NB images at QSOs. In the next section we discuss the more extended line emission regions away from the QSOs. Figures 2 to 11 show the images with contour and grey-scale levels chosen to illustrate the main morphological features.

0738+313 (Fig. 2; z=0.63). The QSO is slightly more extended than the stellar image profiles in both *R* and NB. However, no structure can be seen visually, except for a detached [O II] feature discussed in the next section. There are two close faint companions but there is no evidence that they have any physical connection with the QSO.

0903+169 (Figs. 3 and 4; z=0.41). The *R* band QSO profile appears slightly more extended than the stellar profile, consistent with an elliptical host galaxy. In the outer isophotes, the QSO has a faint halo which is extended in the direction of a companion object. The NB images are too noisy to see these effects.

0957+003 (Fig. 5; z=0.91). The *R* band image is unresolved, with the exception of a possible jet-like feature at eight o'clock. The NB image profile is extended, and has "jets" at 7, 2, and 3 o'clock, but not at 8 o'clock.

1022+194 (Fig. 6; z=0.83). The *R* band image is clearly resolved as elliptical with wispy outer filaments. It is not resolved along the short axis. The NB image is also elliptical (with the same orientation), and is more extended. There is a close companion at 5 arcsec which may be interacting, and another (not obviously connected) at 7 arcsec.

1104+167 (Fig. 7; z=0.63). There is no evidence that either the *R* band or NB images are extended.

1151+102 (Fig. 8; z=0.90). Both the *R* band and the NB images are extended when compared with the star image profiles. No structure can be seen in the images.

1253+104 (Fig. 9; z=0.83). The *R* band profile is not extended except in the outer parts where low level signal extends in two opposite directions. The NB image is more noisy and the QSO profile lies between the two best star profiles. Low level outer structure in the NB QSO image is definitely present.

1340+289 (Fig. 10; z=0.91). The *R* band image is not extended in any way. The NB image is also not extended except for a narrow curved "jet" which we discuss below.

1423+242 (Fig. 11; z=0.65). There is no good star image in the frame. Neither the *R* nor NB QSO image is definitely extended in comparison with the weak star images present. There is no faint structure visible in the QSO continuum images, but there is a faint halo in the continuum subtracted NB image.

1510−089 (z=0.36). Neither the *R* nor NB profiles can be seen to be extended, and no faint structure is seen in them. See comments below on the continuum subtracted image.

The main interest in these results is that we have re-

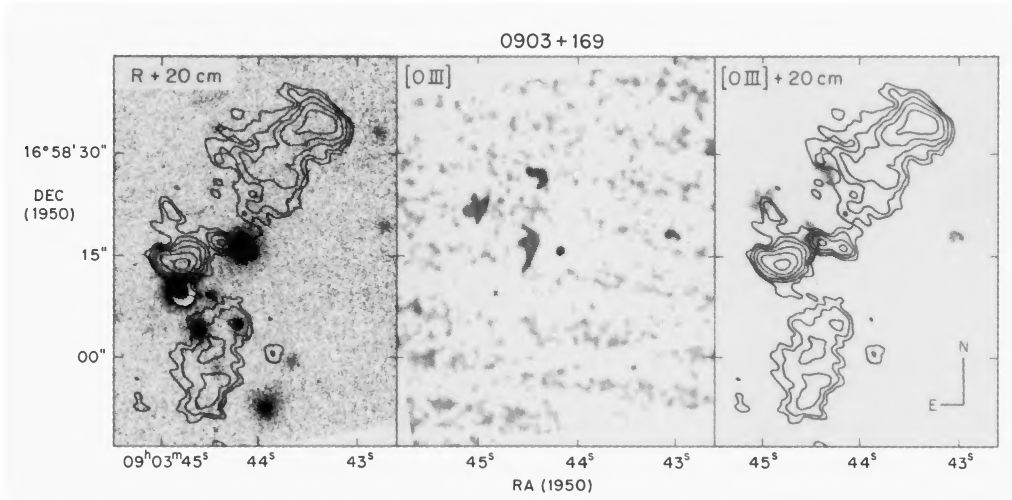

FIG. 4. Images of 0903+169, showing the radio, *R* band, and [O III] structure. The QSO is near the field center and the guide star is to the SE, at the X in the center panel. The image contrast is high to show the [O III] image bright spots.

solved the host galaxy in four QSOs of redshift greater than 0.8. The most clearly resolved of these is 1022+194, and appears to be an elliptical shaped galaxy with no resolved substructure. The size is about 40 kpc, which is comparable with that for resolved RLQSOs at lower redshift. Since the images here are not very deep, we may expect that the structures may be visible to larger radii in longer exposures.

In the sample, we have resolved the QSOs with the faintest nuclei with the best image resolution. There are no inconsistencies to this rule. The unresolved objects all have FWHM of 0.70 or larger, and the low redshift 1510−089 (Z=0.36) is bright (16.5 mag) and its *R* band exposure was half that of the others at 300 s. Therefore, with sufficiently good seeing and image sampling, it appears that QSO host galaxies can be resolved, or at least seen to be extended, to redshifts at least to 0.9.

3. LINE EMISSION

Extended line emission was sought in the vicinity of the QSOs both in the NB image and in the continuum-subtracted NB images. The continuum subtraction was done empirically by scaling the *R* band image until stars (and less rigorously other galaxies) disappeared. The QSO image did not disappear since the nuclear spectra have considerable [O II] and [O III] unresolved emission. A measure of this nuclear or unresolved emission is made by taking the ratio of the *R* and NB signals, scaled to the same exposure. The continuum equivalent values of the three filters used were measured from their transmission curves: 6104A–56A; 6809A–72A; and 7090A–76A. The standard star field gave a mean ratio of 18(±0.6) from *R* band to the 7090A filter, which scales to 19 and 24 for the 6809A and 6104A filters, respectively. Thus, ratios lower than these for the QSO images measure the noncontinuum line emission which is unresolved. Table 2 gives these ratios for all the QSOs, and the factor by which they exceed the continuum signal.

Table 2 also gives a measure of the emission line flux in terms of continuum equivalent. This is the effective *R* band continuum brightness of an object which gives the same NB signal. These numbers are reliable to only 0.5 magnitudes or so, since the seeing was variable, and the continuum band calibration had a scatter of 0.3 mag. The detection limit in the data in these units is about 23–24 mag,

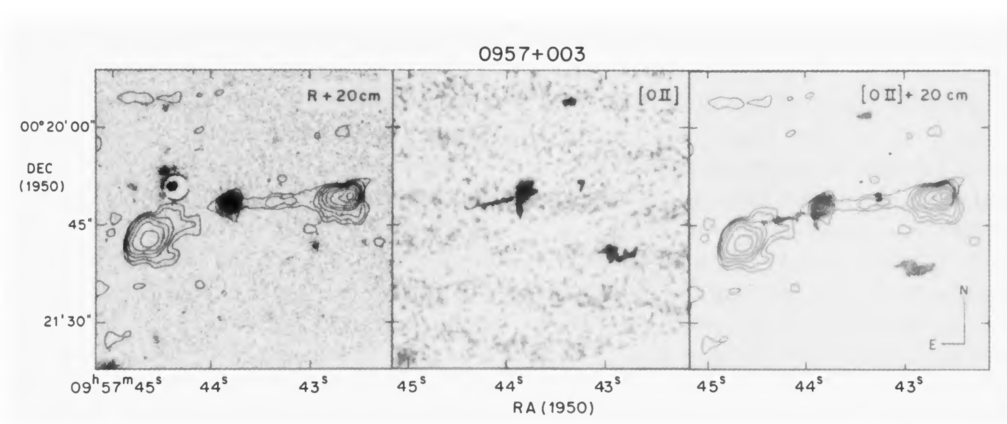

FIG. 5. Images of 0957+003, showing the *R* band, [O II], and radio structure. The image contrast is high to show the [O II] bright areas.

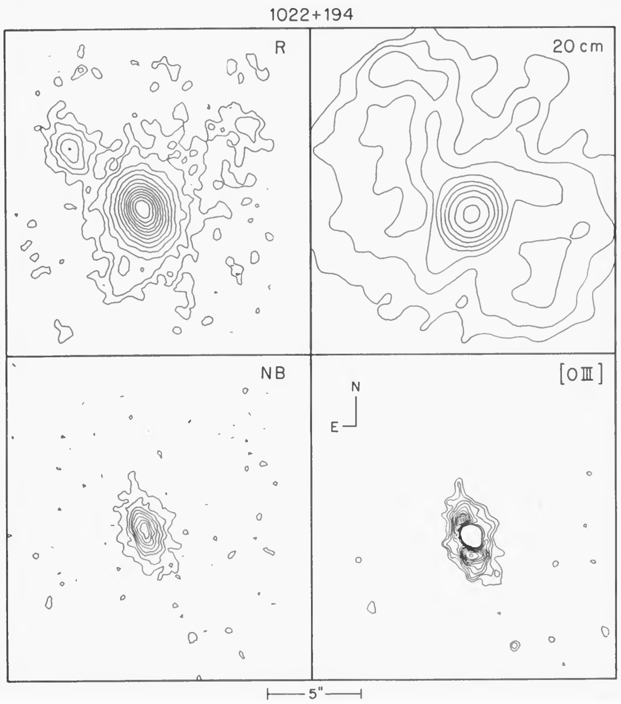

FIG. 6. Images of 1022+194. The R contours are equal ratios; the 20 cm map is from HPG; the NB and [O II] contours are equal intervals. The "hole" in the [O II] image center is due to point-spread function mismatch.

FIG. 8. [O II] image of 1151+102 at high contrast. The QSO is the small spot near the center. The radio source is unresolved at 0.4 arcsec.

depending on the exposure time, seeing and local sky brightness. Since much of the detected emission is faint, the detections are not likely to be complete, and the weakest flux measures are uncertain by a factor of two.

I have attempted to estimate the probability of the emission line detections by sampling the difference and NB images at random. The detections listed in Table 2 and discussed individually below are the high points in the signal in both the raw NB *and* continuum subtracted images, and the probability estimated of the chance that these are random noise fluctuations of this size (typically areas of 600–1500 pixels). In terms of the magnitudes of continuum equivalent in Table 2, the numbers are about 2σ at $m=23$; 3σ at $m=22$, and 4σ at $m=21$. Thus, some of the faint "detections" may be spurious, particularly those that lie a long way from the QSO. Whenever line emission is

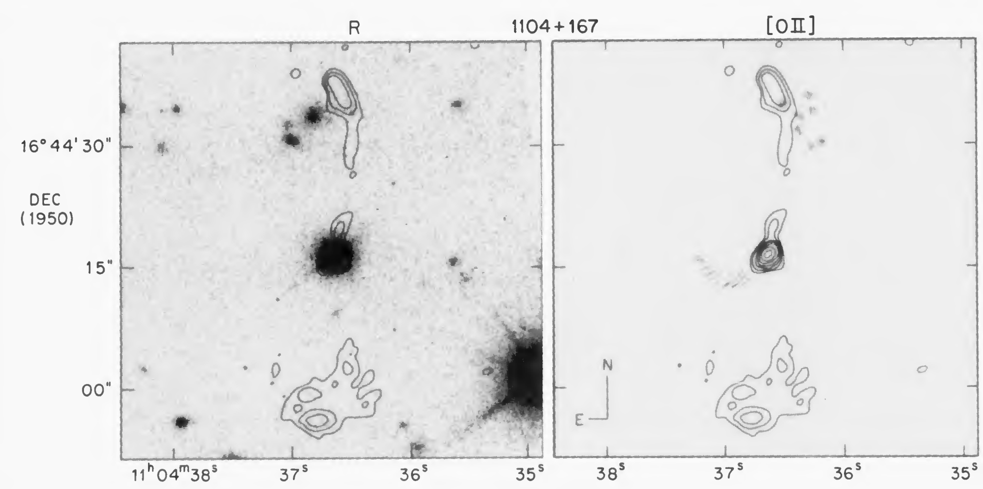

FIG. 7. R band and [O II] images of 1104+167 compared with the radio structure.

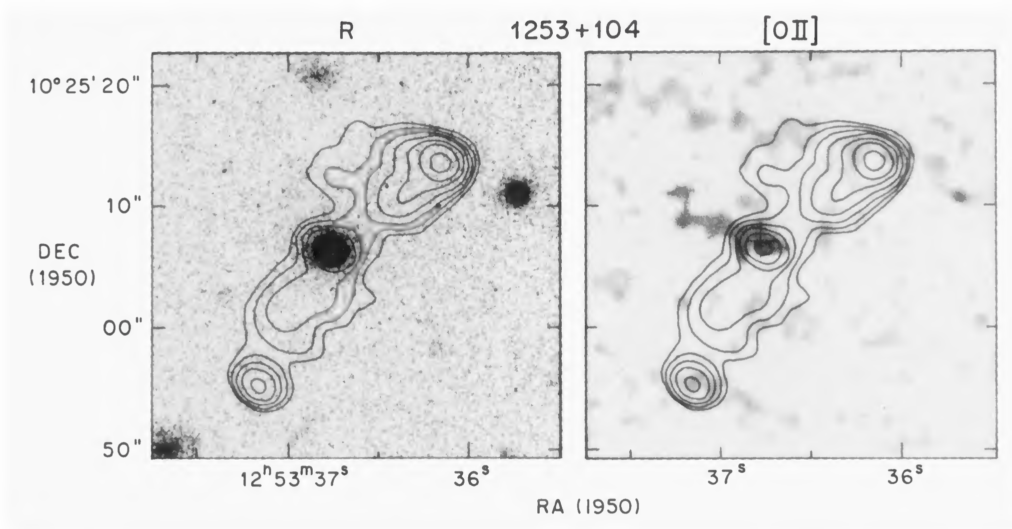

FIG. 9. Images of 1253+104, showing the HPG 20 cm radio structure compared with the R and [O II] images.

detected immediately surrounding the QSO, the signal is quite definite. However, the uncertainties in the strong QSO continuum subtraction make the measurement of these fluxes difficult.

Figures 2 to 11 illustrate the results as clearly as possible for most objects, and comparison with the radio structures from the maps of HPG. The extended line emission is now discussed for each QSO individually.

0738+313. The R band image has telescope support diffraction spikes which are stronger in the 10 o'clock to 4 o'clock direction. In the NB image an extension to the QSO is seen close to the 10 o'clock position. It is not seen at 4 o'clock, and it is broader and at a slightly different angle from the diffraction spike. In the continuum-subtracted image, the feature appears as a detached irregular cloud about 2.4 by 1.9 arcsec, extended azimuthally with respect to the QSO. There is another close companion which is seen in the R band at the same distance at 1 o'clock. This object is not seen in the continuum subtracted image. The feature seems to be a cloud of gas associated with the QSO. The radio source has no structure at the 0.4 arcsec resolution of the very large array.

0903+169. This QSO lies in a cluster studied by Ellingson & Yee (private communication). The radio structure

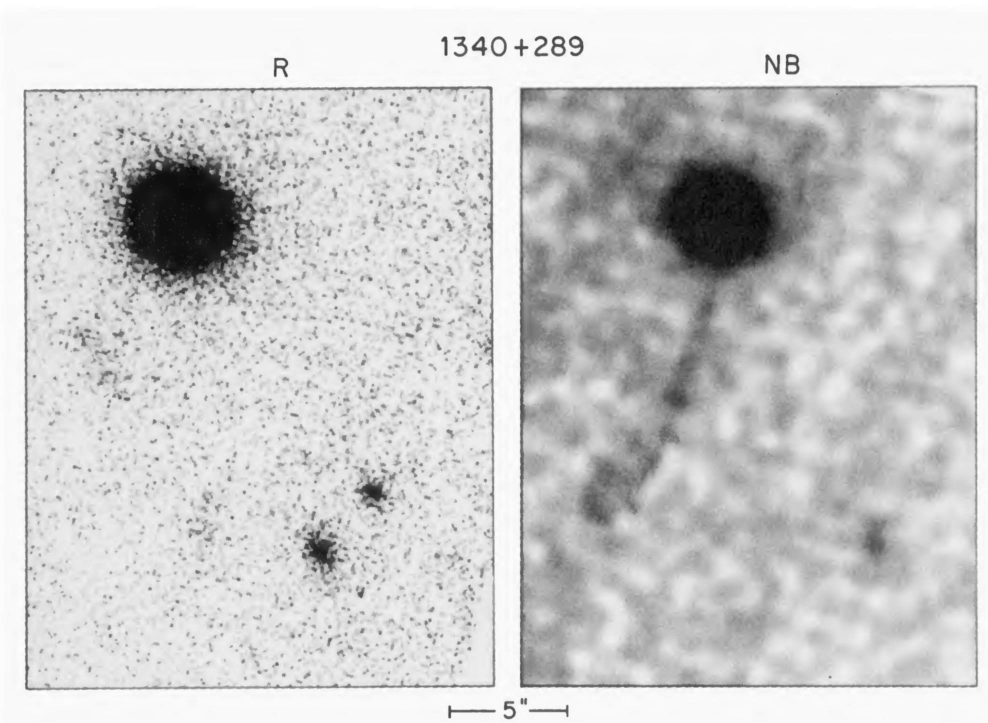

FIG. 10. R and NB images of 1340+289. The one-sided radio structure extends to the SW and lies within the dark part of the optical images.

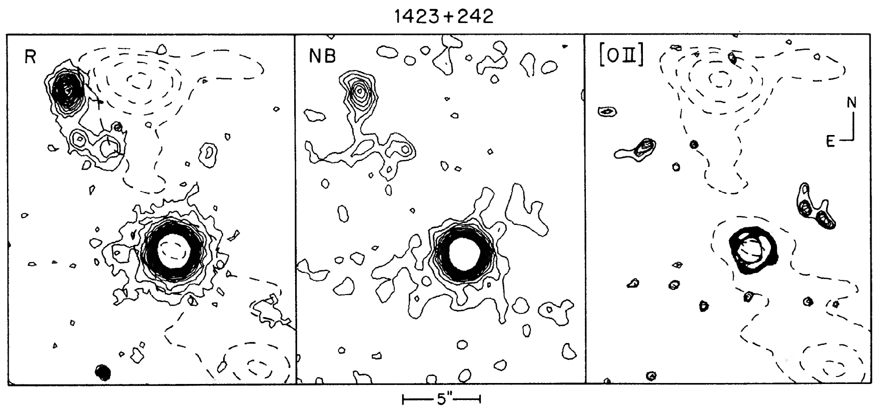

FIG. 11. Images of 1423+242. Dashed contours are the HPG 20 cm radio map. Optical contours are in linear intervals.

is quite large and complex. The shorter radio lobe overlies two of the galaxies nearby, and one bright lobe spot lies on one of these galaxies. There are four clouds of [O II] emission in the area. The closest to the QSO looks like a bow-shock centred on the nearest bright spot in the radio structure which appears to be currently active in this direction. Two other emission line clouds are at the outer edges of parts of both radio lobes, and the last lies away from any radio structure, but along the line opposite to the current radio activity.

The brightest of these clouds is the one near to the QSO, three times brighter than the next which is also in that direction. The cloud not in the radio lobe has the weakest signal. Table 2 gives estimates of the three fluxes.

0957+003. This QSO has a large, slightly bent double-lobe structure. There are several bright areas in the [O II] image, and there is irregular extended line emission around the QSO. The emission near the QSO has one finger along the radio axis, towards the long "jet" lobe, and a major curved extension not along the radio axis. There is a narrow linear emission line region along the radio axis toward and merging with the shorter radio lobe. A possible faint emission knot lies near the bright spot in the radio jet. The other bright regions are unconnected with the radio structure or any other object in the field.

The brightest region is that close to the QSO. The others are of comparable weak signal, and are difficult to measure because of the low level background pattern. Table 2 gives the flux near the QSO, and the total.

TABLE 2. Line emission.

Name	Nuclear.. R/NB	factor[a]	Extended.... Size(")	Mag[b]	Remark
0738+313	13	1.8	4	22.3	irregular cloud; radio unresolved
0903+169	13	1.4	5,10,13	21.3,22.4,22.9	knots in complex lobe, comp. galaxy
0957+003	12	1.5	7,10,3	21.6,Σ21.1	knot + short lobe
1022+194	17	1.1	±3	>18.2(20.6)	line emission extended along radio axis
1104+167	17	1.4	15-22	20.7,21.6	clouds at jet-side lobe; plume
1151+102	16	1.1	3.9,1.2,2.6	22.6,Σ22.0	ext host + filaments; radio unresolved
1253+104	17	1.1	9	21.2	jet perp to radio axis
1340+289	12	1.5	~10	22.6	curved jet 55° to radio axis
1423+242	13	1.8	3,9	20.3,22.9	halo and cloud perp to radio axis
1510−089	18	1.1	7	23.2	weak tail 135° to radio axis

[a] unresolved line emission over continuum

[b] continuum-equivalent R magnitude of line emission. ($23=2\sigma;22=3\sigma;21=4\sigma$)

1022+194. The radio structure is a diffuse halo about 20 arcsec in diameter. There is a long axis, with brighter areas along its length, but no FR II type hotspots. There is bright line emission only immediately surrounding the QSO, with structure extended along the same direction as the continuum, which is also along the radio axis. A faint companion galaxy lies along the radio axis too, within the radio halo, and has no detectable line emission. There is also a faint continuum extension perpendicular to the radio axis, which may be another faint companion or a tidal tail. There is no line emission from this either. Table 2 gives an upper limit and best estimate of the line flux.

1104+167. The radio structure is double-lobed of equal length with a core jet. There are three faint galaxies near the jetted lobe side, and there are several knots of line emission in this region, which may be the peaks of a large cloud that lies along the inner side of the jetted lobe. A very weak curved plume is seen in the NB image, perpendicular to the radio axis, which could be tidal. The detection of this feature is marginal, and the flux is very uncertain. The flux in Table 2 is the sum of the bright clouds seen, and the plume.

1151+102. This is an unresolved radio source. There are three emission line clouds near the QSO, in an elongated distribution on both sides of the QSO. The QSO itself has extended emission along this axis. There are some faint galaxies further away but the clouds have no continuum flux. Table 2 gives the host galaxy and the total emission flux.

1253+104. This is a classical FR II radio source. There is no line emission detected associated with any of the radio structure. However, there is a linear emission line feature which is close to perpendicular to the radio axis, extending about 8 arsec from the QSO. A nearby galaxy 17 arcsec away does not disappear in the continuum subtraction, and may have line emission at this redshift.

1340+289. The radio structure is small and one-sided, only 2.5 arcsec long. There is no detectable emission line structure on this scale, or on larger scales in this direction. However, the NB image does show a remarkable smoothly curved jet at 55° to this direction. The jet extends from the nucleus for 8 arcsec to a bright spot, and then appears to continue smoothly and fainter to 14 arcsec, where it merges with the detector background pattern. This resembles a tidal tail, and is reminiscent of the tail seen in [O III] in 2305+187 (Shara *et al.* 1985).

1423+242. The radio source is a slightly bent weak FR II source. The QSO has several faint extended companions. The brightest of these has two irregular companions between it and the QSO. There is weak line emission from this region, which does not appear to be associated with any of the radio structure. There is some extended line emission close to the QSO, with no predominant direction. Table 2 gives the flux near the QSO, and the distant cloud.

1510−089. This is a small one-sided radio source with a very weak lobe, about 10 arcsec from the core. There is no line emission from this region at all. The continuum-subtracted image shows extended host galaxy emission that extends a few arcsec towards the radio lobe, but this may be an artifact of a small mismatch between the *R* and NB point-spread functions. A weak region of line emission does extend from the QSO 135° away, which could be another curved tidal tail. It is very weak, but lies in a region of low pattern background. There is no definite extension of the QSO line emission.

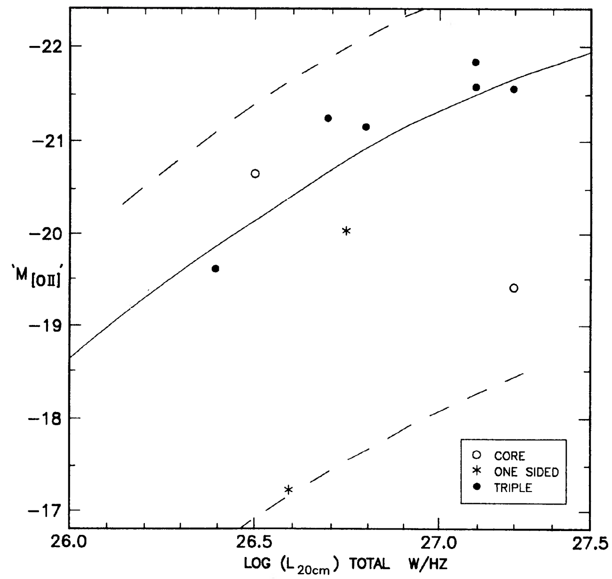

FIG. 12. Plot of line emission and radio luminosity, showing radio morphology types. The optical luminosities are absolute magnitudes of continuum-equivalent emission line fluxes. 10^{27} W/Hz is about 10^{45} erg s^{-1}; $M_R=-24$ is about 10^{44} erg s^{-1}. The lines show the mean and limits of the McCarthy and van Breugel results for radio galaxies, which cover a wider range of luminosity.

4. DISCUSSION

Large-scale line emission is detected in all of these QSO fields, at the QSO redshift. (There is, of course, a chance that the emission is another line at different redshift: this seems unlikely enough to ignore.) There is a wide variety of radio structure and power and also a wide variety of emission line morphology. The emission line structure occurs in three varieties: extended emission contiguous with the host galaxy; jets emerging from the host galaxy; and separate clouds of emission, which may lie very far from the host galaxy. In this small sample, a typical QSO has more than one of these types of emission.

There is some connection with the large-scale radio structure, as seen in the high redshift steep spectrum powerful radio galaxies. In four of the six large triple sources, we have line emission which is aligned or connected with the large-scale radio structure. The line emission is found at the edges—inner and outer—of the radio lobes, and in the two clear cases it is on the shorter (currently active?) lobe. This supports the idea that the line emission may be caused by compression or entrainment of the IGM by the radio material ejected by the nucleus. We do not see any very large emission line sources, such as the median of 80 kpc quoted by McCarthy (1991) for radio galaxies with comparable fluxes.

In the two large sources that do not show lobe-connected emission, there is line emission from the immediate surrounding of the host galaxy. Such "local" line emission is seen in five (possibly six) objects, and is similar to that found in the low redshift objects by Stockton and MacKenty. The fraction of QSOs which show this is comparable to the ~50% found by them. In only one (possibly two) of these is the emission line region pointing at the radio structure, and even there, it is not the principal extension seen. Thus, the directional connection is weaker than in the results of McCarthy *et al.* (1991).

We also see some examples of jets or tidal tails that are not connected with the radio and are not irregular as the local clouds. These are presumably ionized by the QSO nucleus. The most striking of these is 1340+289. These are not common in low redshift emission line objects, and may require to be illuminated by a powerful radio or optical source not common at low redshift. Hutchings & Neff (1992) have reported several jet-like phenomena in high resolution continuum images of low-redshift QSOs. Gas jets and tails are QSO phenomena not yet well understood. [Note that there is a low redshift example of a tail in 2305+187 by Shara *et al.* (1985), and Hutchings *et al.* (1992), but not confirmed by Stockton & MacKenty (1987).]

Figure 12 shows the sum of the emission line (continuum-equivalent) luminosity plotted against the total radio power. The line luminosity is given in "absolute magnitude" derived from the equivalent magnitudes in Table 2 and $H_0=100$, $q_0=0.5$. As a rough conversion a radio luminosity of 10^{27} W/Hz is 10^{45} erg s^{-1}, and $M_R=-24$ is 10^{44} erg s^{-1}. As found by others, the large lobe-dominated (steep spectrum) sources have larger emission line luminosity than the compact (flat spectrum) sources. In most cases, the emission line luminosity is principally in the flux from the immediate surrounding of the QSO, and not from the distant clouds. For most sources the emission line luminosity is correlated with the total radio luminosity, as noted by McCarthy (1992), suggesting that the two are coupled. Using the above conversions of units, the data from this paper fit well with the radio-galaxy results of McCarthy and van Breugel, as sketched in Fig 12. The correlation is weaker for the core flux only, indicating that the radio lobes also play a part in the line emission. However, the emission line luminosity varies with the core spectral index, in the sense that the flat spectrum objects have stronger emission line flux. This also suggests a connection with the strength of the nuclear source.

Finally, in this connection, we find that the unresolved nuclear line emission (as derived from column 3 of Table 2) correlates with the total radio power, again stressing the connection between the line emission and the nuclear source. This correlation is not evident between the extended and nuclear line emission.

The unresolved and small one-sided radio sources have lower emission line luminosity than the large lobe-dominated sources (although 1022+194 is slightly core dominated). If the evolution of the individual sources is measured by size and core dominance, as suggested by Neff & Hutchings (1990), then the evolution of line emission luminosity may accompany the radio in two ways. First, the lobes interact with the IGM and produce extra optical radiation, and second, the radio jets or fueling history of the nucleus clear the nuclear environment of obscuring material so that the ionizing radiation illuminates the gas clouds in the outer parts of the host galaxy.

In general, the detached emission line clouds are less luminous and less extensive than found in high redshift radio galaxies. In both radio galaxies and QSOs, there is strong suggestion from the linear nature of the line emission region morphology, that they are illuminated by beamed or collimated radiation from the nucleus, in the cases where they do not lie in the radio lobes. We also have several cases where the direction of illumination is different from the radio axis. It would be interesting to know whether this is a circumstance that changes during the lifetime of individual sources, due perhaps to clearing of the host galaxy dust, a change of the nuclear orientation, or even binary nuclei.

There is only one example of a nearby galaxy showing line emission (1423+242). This too may reflect on the beamed nature of the ionizing radiation. However, in this connection we note that Yanny & York (1992) claim to see faint emission line regions in dense environments at redshifts 0.6 and higher. While their detection limits are fainter than those in this paper, we note that QSO environments at these redshifts may also contain such regions, which would presumably not be associated with the QSO activity.

The continuum resolution of the host galaxies indicates that there is no strong evolution of the nature of the hosts above redshift 0.5. This too is different from what is found for radio galaxies, which appear to be larger and more irregular at higher redshift.

A more extended study of the range of radio source types and redshifts is clearly needed to put any of these results on a statistical basis. Also, deeper line emission imaging would be desirable. Since these studies are one of the few ways of studying structure at high redshifts, the substantial amount of observing time required would be a good investment.

I thank P. Hickson for the use of the NB filters.

REFERENCES

Ellingson, E., & Yee, H. K. C. 1992, private communication
Heckman, T. M., Lehnert, M. D., van Breugel W., & Miley, G. K. 1991, ApJ, 370, 78
Hutchings, J. B., & Neff, S. G. 1992, AJ, 104, 1
Hutchings, J. B., Crabtree, D., Neff, S. G., & Gower, A. C. 1992, PASP, 104, 66
Hutchings, J. B., Price, R., & Gower, A. C. 1988, ApJ, 329, 122 (HPG)
McCarthy, P. J. 1991, ASP Conference (preprint)
McCarthy, P. J., van Breugel, W., & Kapahi, V. K. 1991, ApJ, 371, 478
McClure, R. D. *et al.* 1989, PASP, 101, 1156
Neff, S. G., & Hutchings, J. B. 1990, AJ, 100, 1441
Shara, M. M., Moffat, A. F. J., & Albrecht, R. 1985, ApJ, 296, 399
Stockton, A. & MacKenty, J. W. 1987, ApJ, 316, 584
Yanny B., & York, D. G. 1992, preprint